J Mater Sci (2007) 42:633–639
DOI 10.1007/s10853-006-1144-y

Role of dynamic strain aging in corrosion fatigue of low-alloy pressure vessel steel in high temperature water

X. Q. Wu · Y. Katada

Received: 4 August 2004 / Accepted: 17 November 2005 / Published online: 22 November 2006

Abstract Low cycle fatigue (LCF) behavior of an A533B-type low-alloy pressure vessel steel was investigated in 200 °C and 288 °C water. Major attention was paid to the role of dynamic strain aging (DSA) on corrosion fatigue behavior of the steel. It was found that DSA played a noticeable role in the present corrosion fatigue process, manifested by the strain-rate and temperature dependent cyclic stress and plastic strain amplitude response. DSA was found to occur at a low strain rate in 200 °C water or at a high strain rate in 288 °C water regardless of dissolved oxygen concentration (DO) in water. In low-DO water, DSA improved the LCF resistance of the steel to some extent, but such an effect was screened by the environmental effects in high-DO water. The interactions between DSA and surrounding environmental factors as well as their possible influence on environmentally assisted cracking and fatigue resistance of the steel in high temperature water are discussed.

X. Q. Wu (✉)
Environmental Corrosion Center, Institute of Metal Research, South Campus, 62 Wencui Road, Shenyang 110016, P.R. China
e-mail: xqwu@imr.ac.cn

Y. Katada
Corrosion Resistant Design Group, Steel Research Center, National Institute for Materials Science, 1-2-1, Sengen, Tsukuba, Ibaraki 305-0047, Japan

Introduction

Dynamic strain aging (DSA) has been reported to occur in many materials during monotonic tensile deformation in a specific range of strain rate and temperature as a result of the interactions between diffusing solute species and mobile dislocations [1–10]. DSA is also found to significantly affect other properties of steels and alloys such as fatigue resistance [11–21], drawability [22] and abrasion resistance [23]. However, most of previous studies on this area were focused on the pure mechanical effects of DSA on material properties rather than the interactions between DSA and surrounding environments. Low-alloy steels such as ASTM A508, A533 and their equivalent materials have been extensively applied in fabricating pressure boundary components in nuclear power plants worldwide. Basically these steels cannot be immune from the effects of DSA in their service environments. It is thus of great significance to investigate the influence of DSA on the mechanical properties of these steels in their service environments.

The present work is to investigate the low cycle fatigue (LCF) behavior of an A533B-type low-alloy pressure vessel steel in high temperature water. Major attention was paid to the roles of DSA on corrosion fatigue behavior of the steel. It is expected to clarify the underlying interactive mechanism between DSA and high-temperature water environments.

Experimental

A hot-rolled A533B-type low-alloy steel plate was used for the present study. The chemical composition

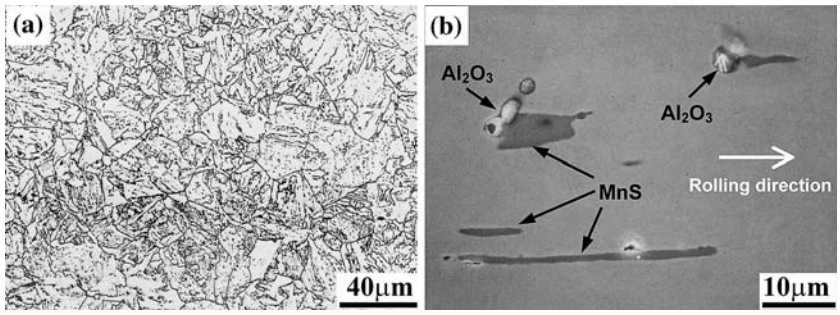

Fig. 1 Microstructure and inclusions in the steel. (**a**) upper bainite, (**b**) MnS and Al_2O_3 inclusions

(wt.%) was 0.17 C, 0.24 Si, 0.36 Mn, 0.003 P, 0.038 S, 0.59 Ni, 0.009 Cr, 0.47 Mo, 0.007 Co, 0.023 Al, <0.005 Cu, <0.003 V, 31 ppm N, <10 ppm O, and balance Fe. The as-received microstructure was upper bainite as shown in Fig. 1a. The inclusions in steel mainly consisted of MnS with elongated morphology along the rolling direction, accompanying a few of Al_2O_3 (Fig. 1b). The volume fraction of inclusions is about 0.163%.

Round-bar specimens with 8 mm gauge diameter and 16 mm gauge length were machined from the steel plate along the rolling direction. The experimental equipments for the fatigue tests in high temperature water were similar to those used previously [24]. LCF tests were conducted in a strain-control mode with a fully reversed triangular waveform. The water chemistry was controlled as 100 or 2,000 ppb dissolved oxygen concentration (DO), 6.2–6.5 pH value and <0.2 μS/cm conductivity. The pressure of high temperature water was fixed at 8.0 MPa during the tests. Fatigue life, N_{25}, was defined as a number of cycles at which the peak tensile stress descended to 75% of the level of the maximum peak stress.

Some tested specimens were broken apart in liquid nitrogen. The fatigue fractures were examined using a scanning electron microscope equipped with an energy dispersive X-ray spectrometry.

Results

Figure 2 shows the dependence of stress amplitude on the number of cycles in high temperature water. At 200 °C, greatly distinguished stress amplitude response occurred at different strain rates (Fig. 1a). A distinct softening took place at a high strain rate (0.1% s^{-1}), while a relatively stable stress amplitude response or a slight secondary hardening appeared at a low strain rate (0.001% s^{-1}). Such difference in stress amplitude response seemed to increase with an increase in applied strain amplitude, namely, the secondary hardening at a low strain rate appeared more remarkable under the high strain amplitude condition (0.75% as arrowed in Fig. 2a). At 288 °C, however, the stress amplitude responded almost similarly at different strain rates, showing a relatively stable behavior or a slight secondary hardening (Fig. 2b). Distinguished from that at 200 °C, a slight softening took place at the low strain rate (0.001% s^{-1}) rather than the high strain rate (0.1% s^{-1}). Such a softening also became more obvious under the high strain amplitude condition. Table 1 lists the stress amplitude and plastic strain amplitude obtained from the stabilized hysteresis loops at half of fatigue life. At 200 °C, a lower plastic strain amplitude and a higher stress amplitude appeared at the low strain rate, while at 288 °C, a lower plastic strain amplitude and a higher stress amplitude appeared at the high strain rate, in particular under the high strain amplitude condition. Increasing DO from 100 ppb to 2,000 ppb seemed to have little influence on the stress amplitude response. The softening still happened at the high strain rate at 200 °C, while a relatively stable stress amplitude response or a slight secondary hardening appeared at the low strain rate at 200 °C or at both low and high strain rates at 288 °C (Fig. 2c).

Figure 3 shows the relationship between the fatigue life and applied strain amplitude in high temperature water. Decreasing strain rate remarkably degraded the LCF resistance of the steel regardless of the testing temperatures and DO in water. In 100 ppb DO water (Fig. 3a), the fatigue resistance at the high strain rate (0.1% s^{-1}) at 200 °C was a little worse than that at 288 °C, while the fatigue resistance at the low strain rate (0.001% s^{-1}) at 200 °C was to some extent better than that at 288 °C, especially under the high strain amplitude condition. In 2,000 ppb DO water (Fig. 3b), the LCF resistance at both low and high strain rates at 200 °C was much better than that at 288 °C.

Figure 4 shows typical fatigue fracture morphologies obtained at different strain rates in 288 °C water (DO = 100 ppb). At the high strain rate (0.1% s^{-1}), a rough fracture was obtained (Fig. 4a), on which typical hydrogen-induced cracking features such as fan-like

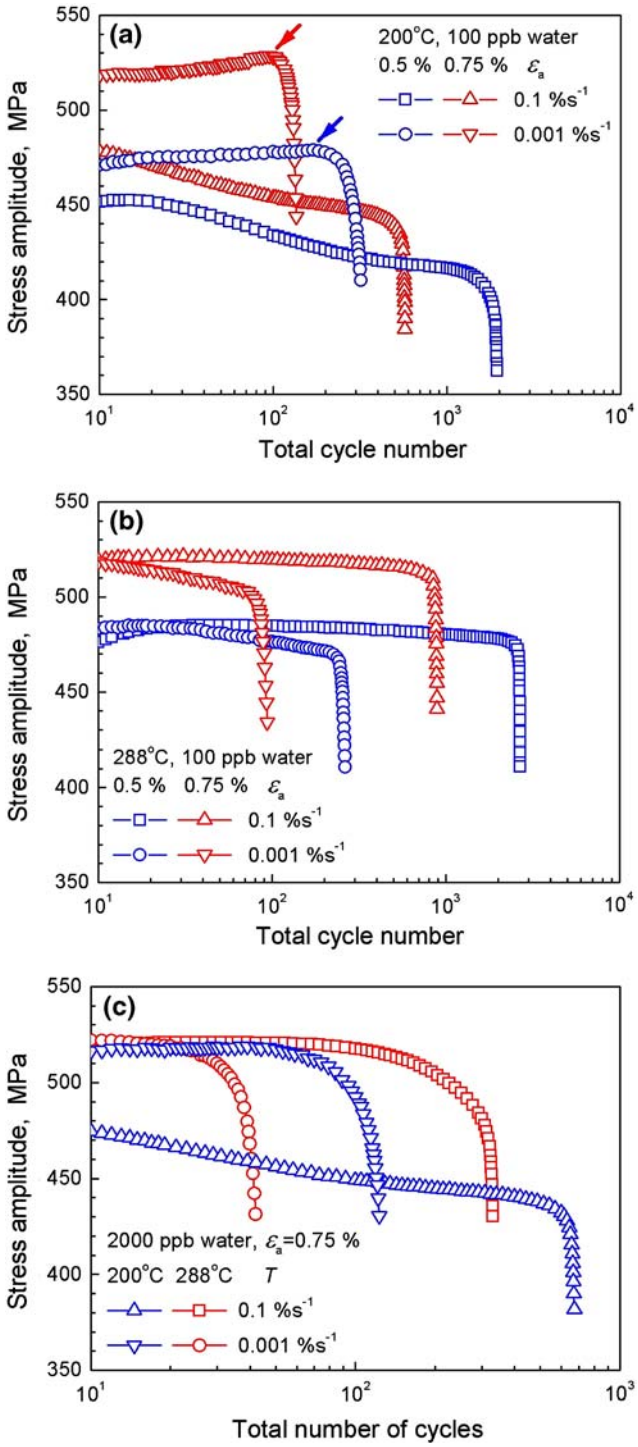

Fig. 2 Dependence of stress amplitude on the number of cycles in high temperature water. (**a**) DO = 100 ppb, 200 °C, (**b**) DO = 100 ppb, 288 °C, (**c**) DO = 2,000 ppb

patterns, tear ridges and terraced cracking morphologies, were frequently observed, especially around or near the MnS inclusions (Fig. 4b). At the low strain rate (0.001% s^{-1}), however, a relatively flat fracture was obtained (Fig. 4c), on which no typical hydrogen-induced cracking feature was observed (Fig. 4d). Similar fatigue fracture morphologies were observed in 2,000 ppb DO water and showed similar strain-rate dependence.

Discussion

The stress amplitude response described above suggested that DSA played a sure role in the present LCF process in high temperature water, which could be proven by following evidences. Firstly, the stable stress amplitude response or slight secondary hardening observed at the low strain rate at 200 °C and at both low and high strain rates at 288 °C (Fig. 2) indicated that some additional strengthening factors existed during the cyclic deformation in high temperature water, which should be attributed to the effects of DSA as proposed by Abdel-Raouf et al. [11]. Lee et al. [15] also reported a similar saturated hardening or a slight secondary hardening due to DSA for A508 steel fatigued in high temperature air. Regarding the stress amplitude response (Fig. 2), stronger DSA effects occurred at the low strain rate at 200 °C or at the high strain rate at 288 °C. Secondly, the above stable stress amplitude response or secondary hardening was susceptible to the testing temperature. A distinct softening occurred at the high strain rate (0.1% s^{-1}) at 200 °C, while a slight hardening appeared at the same strain rate at 288 °C. This is consistent with the typical DSA behavior, namely, the higher the temperature, the larger the strain rate for the onset of DSA [1–4]. Finally, the stabilized cyclic stress amplitude and plastic strain amplitude at half of fatigue life (Table 1) depended not only on strain rate, but also on applied strain amplitude. At 200 °C, a lower plastic strain amplitude and a higher stress amplitude appeared at the low strain rate, while at 288 °C, a lower plastic strain amplitude and a higher stress amplitude appeared at the high strain rate, especially under the high strain amplitude condition. This is in good agreement with the typical DSA behavior that DSA occurs only in special temperature and strain-rate regimes and is also closely dependent on the applied strain [10, 15, 25–27]. Moreover, the stress amplitude at 200 °C, which showed a negative strain-rate sensitivity (i.e., a higher stress amplitude appeared at a lower strain rate during cyclic deformation), is another typical DSA manifestation [2, 20, 25].

Although the effects of DSA on fatigue life of steels have been frequently investigated during past several decades [11–21], there still remains some controversy on this aspect. Previously Abdel-Raouf [11] found that

Table 1 The stress amplitude and plastic strain amplitude at half of fatigue life (DO = 100 ppb)

		200 °C		288 °C	
		0.1% s^{-1}	0.001% s^{-1}	0.1% s^{-1}	0.001% s^{-1}
Stress amplitude σ_a, MPa	ε_a = 0.5%	411.63	477.67	473.18	472.19
	ε_a = 0.75%	448.68	527.56	515.99	506.62
Plastic strain amplitude ε_{ap}, %	ε_a = 0.5%	0.238	0.184	0.186	0.192
	ε_a = 0.75%	0.492	0.420	0.412	0.435

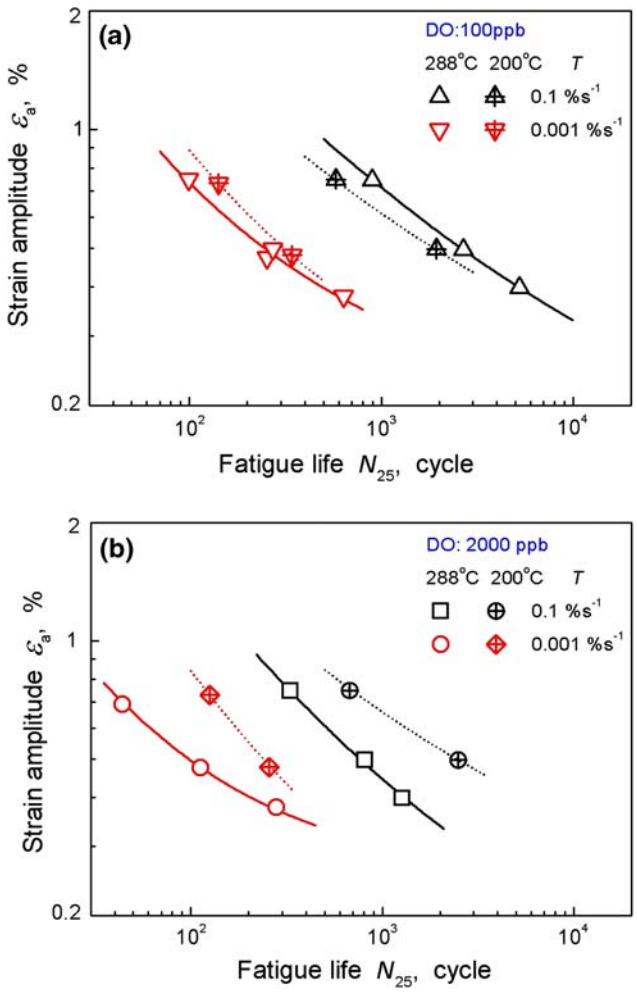

Fig. 3 The relationship between the fatigue life and applied strain amplitude in high temperature water. (**a**) DO = 100 ppb, (**b**) DO = 2,000 ppb.

the fatigue life of Ferrovac E iron (0.007 wt.%C) did not vary with the strain rate except for the DSA region and the shorter fatigue life resulted from DSA. Tsuzaki et al. [12] reported that DSA induced a large decrease in fatigue life in a pearlitic eutectoid steel. Weisse et al. [13] found that a maximum DSA resulted in a maximum fatigue life in stress-controlled tests for low carbon steel SAE 1045, while a minimum fatigue life in plastic-strain-controlled tests. The primary reason for the decrease in fatigue life was usually attributed to the marked cyclic hardening due to DSA. It was believed that higher response stresses developed during the cyclic deformation can lead to a larger stress concentration at the crack tip, which would increase the crack growth rate and hence reduce the number of cycles at the stage of crack propagation. However, some other authors reported a different result. Lee et al. [15] found that the fatigue life of A508 Cl.3 steel in the DSA region increased markedly. They argued that DSA promoted the crack initiation by enhancing local deformation inhomogeneity, but retarded the crack propagation by both promoting crack branching and suppressing the plastic zone ahead of the crack tip. Because the crack initiation life was much shorter than the crack propagation life in the LCF, total fatigue life can be increased by DSA. Recently Huang et al. [21] also reported that the combined effects of DSA and grain size reduction were responsible for the better fatigue resistance of A533 pressure vessel steels, which was attributed to an improved steel strength.

In the present study, under the low-DO condition (100 ppb), the LCF resistance of the steel at the high strain rate (0.1% s^{-1}) in 200 °C water was lower than that in 288 °C water, while the LCF resistance at the low strain rate (0.001% s^{-1}) in 200 °C water was better than that in 288 °C water, especially under the high strain amplitude condition (Fig. 3a). This suggested that some extra strengthening factors existed during cyclic deformation at the low strain rate in 200 °C water or high strain rate in 288 °C water and can be rationalized by the effects of DSA. As mentioned above, DSA appeared more strongly at the low strain rate at 200 °C or high strain rate at 288 °C. It has been reported that the DSA can enhance the fatigue resistance of low-alloy steels in high temperature air [15, 21]. The similar effects of DSA are believed to play an important role in the present LCF process in low-DO water. However, under the high-DO condition (2,000 ppb), the LCF resistance of the steel in 288 °C water was much lower than that in 200 °C water regardless of strain rate (Fig. 3b). This indicated that

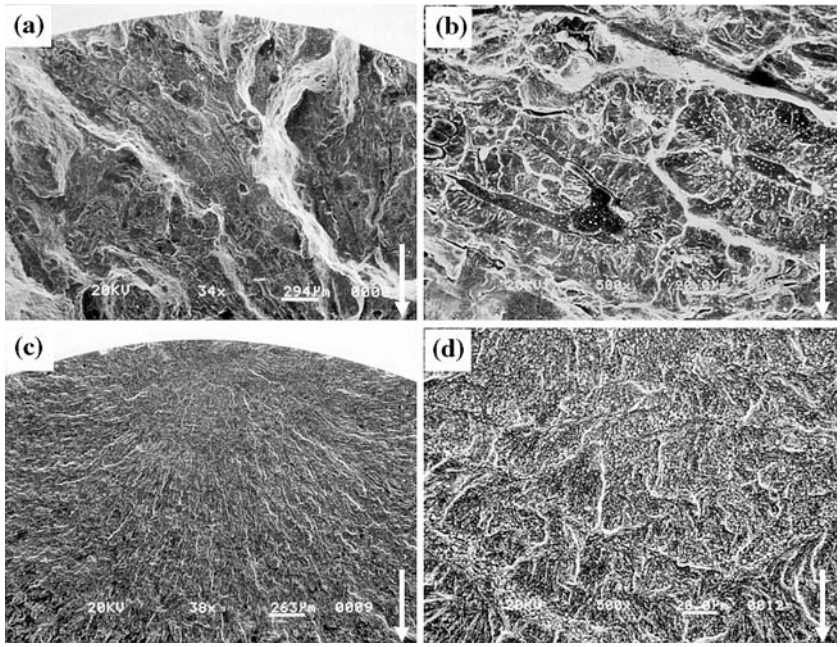

Fig. 4 Typical fatigue fracture morphologies obtained at different strain rates in 288 °C water, arrows show the crack growth direction. (**a**) 0.1% s^{-1}, (**b**) high-magnification morphology of (**a**), (**c**) 0.001% s^{-1}, (**d**) high-magnification morphology of (**c**)

the environmental factors played a more important role on the fatigue resistance than the DSA. By comparing Fig. 3a and b, it was clear that the degradation in LCF resistance in high-DO water mainly took place at 288 °C, while little change occurred at 200 °C. This suggested that the environmental effects may become heavily significant in a special DO-temperature-combined region and screen the effects of DSA. Several previous studies also found that DSA only played a relatively important role in the environmentally assisted cracking (EAC) in less aggressive environments [4]. A good coincidence was observed between DSA behavior and stress corrosion cracking in the water with DO below or equal to 400 ppb [28].

It should be noted that most of the previous studies were focused on the pure mechanical effects of DSA and little attention was paid to the interactions between DSA and surrounding environments. During cyclic deformation in high temperature water, strain localization such as Lüders or PLC (Portevin and Le Chatelier) bands may be induced by DSA [25, 29, 30] in the areas ahead of the crack tips. The strain localization promotes the formation of extrusions and intrusions at metal surface of the crack tips [20]. This undoubtedly accelerates the rupture of oxide films at the crack tips, in turn promotes following metal (M) dissolution reaction at the crack tips,

$$M \rightarrow M^{n+} + ne^{-} \tag{1}$$

In this regard, DSA may promote the EAC due to enhancing the metal dissolution at the crack tips. Moreover, the enhanced metal dissolution promotes subsequent hydrolysis reaction (2), accomplished by the hydrogen reduction reaction (3) at the crack tips or oxygen reduction reaction (4) usually near the crack mouth.

$$M^{n+} + pH_2O \rightarrow M(OH)_p^{(n-p)+} + pH^{+} \tag{2}$$

$$H^{+} + e^{-} \rightarrow H_{abs} \tag{3}$$

$$pO_2 + 2pH_2O + 4pe^{-} \rightarrow 4pOH^{-} \tag{4}$$

The reaction (2) lowers the pH value in solution in the crack-tip area and the reaction (3) may promote the development of hydrogen-induced cracking ahead of the crack tip. Actually hydrogen embrittlement was found to be involved in the present corrosion fatigue process in high temperature water. Typical hydrogen-induced cracking features (Fig. 4b) were observed on the fatigue fracture surface at the high strain rate (0.1% s^{-1}). A special attention, therefore, should be paid to the possible interactions between DSA and hydrogen embrittlement. The DSA-induced localized strain structure has been proved to be a preferred trap for hydrogen [31]. So the hydrogen prefers to concentrate in the strain localization zones if they could enter the metal matrix ahead of the crack tip. The enriched hydrogen also enhances the localization of plastic deformation by promoting dislocation multiplication and motion [32]. As a result, much more severe strain localization ensues ahead of the crack tip due to the combined action between DSA and

hydrogen. This not only enhances the rupture of oxide films at the crack tips, but also increases the stress concentration at internal interfaces (such as inclusion/matrix and carbide/matrix interfaces) where local stresses are expected to develop due to plastic incompatibilities and dislocation pile-ups. Consequently, both metal dissolution at the crack tip and the crack initiation and growth ahead of the crack tips may be enhanced. Recent work [9, 33–35] also indicated that a synergism of DSA and hydrogen embrittlement existed in high-temperature aqueous environments and may promote EAC. At the low strain rate (0.001% s^{-1}), no typical hydrogen-induced cracking features appeared on the fatigue fracture surface (Fig. 4d). This is believed to be due to a change in dominant EAC mechanism from hydrogen-induced cracking at a high strain rate to slip-dissolution-controlled cracking at a low strain rate [36–38]. Although the interactions between DSA and hydrogen become relatively weak, the effects of DSA on the metal dissolution at the crack tip still remains. The DSA-enhanced EAC, therefore, may occur even at a low strain rate in high-temperature water environments.

In view of the above results, it seems that DSA has a two-way effect on the fatigue resistance of the steel in high-temperature water environments. On the one hand, DSA tends to improve the fatigue resistance of the steel by either retarding the fatigue crack propagation or strengthening the steel. On the other hand, DSA interacts with the surrounding environmental factors and enhances the EAC. It is believed that the above two effects of DSA compete with each other in the corrosion fatigue process in high temperature water, and which one is dominant depends on the aggressive degree of environments. As a result, the fatigue resistance of the steel in less aggressive environments (such as low-DO water) was improved to some extent due to DSA, while it was remarkably degraded in more aggressive environments (such as high-DO and high temperature water) by synergistic actions of DSA and surrounding environmental factors.

Conclusions

1. DSA played a noticeable role in corrosion fatigue process of low-alloy pressure vessel steels in high-temperature water environments, manifested by the strain-rate and temperature dependent cyclic stress and plastic strain amplitude response. In the present study, DSA was found to occur at a low strain rate in 200 °C water or at a high strain rate in 288 °C water regardless of DO in water.
2. LCF resistance of the present steel in high temperature water degraded remarkably with a decrease in strain rate regardless of testing temperature and DO in water. DSA was found to improve the LCF resistance of the steel in low-DO water to some extent, but such an effect was screened by the environmental effects in high-DO water.
3. A synergistic effect of DSA and high-temperature water environments may exist during cyclic deformation, in which DSA-induced strain localization promotes the oxide-film rupture and thus metal dissolution at the crack tip. In the hydrogen-induced cracking process, a further interaction between DSA and hydrogen may enhance the EAC.
4. It is believed that DSA has a two-way effect on the fatigue resistance of low-alloy pressure vessel steel in high-temperature water environments. On the one hand, DSA tends to improve the fatigue resistance of the steel by either retarding the crack propagation or improving the steel strength. On the other hand, DSA interacts with surrounding environmental factors and promotes the EAC. The above two effects compete with each other in the corrosion fatigue process, and which one is dominant depends on the aggressive degree of the surrounding environments.

Acknowledgements This study was partially supported by the Innovation Fund of Institute of Metal Research, CAS, the Special Funds for the Major State Basic Research Projects, NSFC (2006CB605000) as well as the Budget for Nuclear Research of the Ministry of Education, Culture, Sports, Science and Technology in Japan. The authors also wish to acknowledge Mr. S. Ohashi and Mr. A. Katayama in NIMS, Japan, for their help in fatigue tests.

References

1. Marschall CW, Landow MP, Wilkowski GM (1990) ASTM STP 1074:339
2. Kubin LP, Estrin Y (1990) Acta Metall Mater 38:697
3. Kang SS, Kim IS (1992) Nucl Technol 97:336
4. Atkinson JD, Yu J (1997) Fat Fract Eng Mater Struct 20:1
5. Seok CS, Murty KL (1999) Int J Press Vess Piping 76:945
6. Rowcliffe AF, Zinkle SJ, Hoelzer DT (2000) J Nucl Mater 283–287:508
7. Hoelze DT, Rowcliffe AF (2002) J Nucl Mater 307:596
8. Gonzalez BM, Marchi LA, Fonseca EJ, Modenesi PJ, Buono VTL (2003) ISIJ Int 43:428
9. Wu XQ, Kim IS (2003) Mater Sci Eng A348:309
10. Zhu SM, Nie JF (2004) Scripta Mater 50:51
11. Abdel-Raouf H, Plumtree A, Topper TH (1973) ASTM STP 519:28
12. Tsuzaki K, Matsuzaki Y, Maki T, Tamura I (1991) Mater Sci Eng A142:63

13. Weisse M, Wamukwamba CK, Christ HJ, Mughrabi H (1993) Acta Metall Mater 41:2227
14. Valsan M, Sastry DH, Rao KBS, Mannan SL (1994) Metall Mater Trans 25A:159
15. Lee BH, Kim IS (1995) J Nucl Mater 226:216
16. Armas AF, Avalos M, Alvarez-Armas I, Petersen C, Schmitt R (1998) J Nucl Mater 258–263:1204
17. Srinivasan VS, Valsan M, Sandhya R, Rao KBS, Mannan SL, Sastry DH (1999) Int J Fat 21:11
18. Herenu S, Alvarez-Armas I, Armas AF (2001) Scripta Mater 45:739
19. Kim DW, Kim WG, Ryu WS (2003) Int J Fat 25:1203
20. Mughrabi H (2003) Z Metallkd 94:471
21. Huang JY, Hwang JR, Yeh JJ, Chen CY, Kuo RC, Huang JG (2004) J Nucl Mater 324:140
22. Taheri AK, Maccagno TM, Jonas JJ (1995) ISIJ Int 35:1532
23. Celik O, Ahlatci H, Kayali ES, Cimenoglu H (2003) ISIJ Int 43:1274
24. Nagata N, Sato S, Katada Y (1991) ISIJ Int 31:106
25. Robinson JM, Shaw MP (1994) Inter Mater Rev 39:113
26. Choudhary BK, Rao KBS, Mannan SL, Kashyap BP (1999) Mater Sci Technol 15:791
27. Gupta C, Chakravartty JK, Wadekar SL, Dubey JS (2000) Mater Sci Eng A292:49
28. Rippstein K, Kaesche H (1989) Corros Sci 29:517
29. Morris JG (1970) Mater Sci Eng 5:299
30. Caceres CH, Rodriguez AH (1987) Acta Metall 35:2851
31. Le TD, Bernstein IM (1991) Acta Metall Mater 39:363
32. Birnbaum HK, Sofronis P (1994) Mater Sci Eng A176:191
33. Wu XQ, Katada Y, Lee SG, Kim IS (2004) Metall Mater Trans 35A:1477
34. Lee SG, Kim IS (2001) J Press Vess Technol 123:173
35. Chu WY, Wang YB, Qiao LJ (2000) J Nucl Mater 280:250
36. Wu XQ, Katada Y (2004) Mater Sci Eng 379A:59
37. Wu XQ, Katada Y (2004) J Mater Sci 39:2519
38. Wu XQ, Katada Y (2005) Corros Sci 47:1415